JOURNAL OF MATERIALS SCIENCE 26 (1991) 6599–6605

Role of recovery in high temperature constant strain rate deformation

O. AJAJA *
Department of Mechanical and Production Engineering, National University of Singapore, Kent Ridge, Singapore 0511

A model based on the three-dimensional distribution of dislocations is used to delineate the role of recovery during high temperature constant strain rate deformation. The model provides a good semi-quantitative explanation for classical work-hardening as well as for high temperature work-softening resulting from rapid recovery. It predicts linear work-hardening, whereby the ratio of the work-hardening rate, H, to the shear modulus, G, is constant when a crystal is tested in the absence of recovery. The slope of the stress–strain curve, θ, for high temperature deformation is related to the low temperature work-hardening rate H; the dislocation annihilation rate $\dot{\rho}_a$, the flow stress σ, the free dislocation density ρ, the strain rate $\dot{\varepsilon}$, and a parameter which is sensitive to the dislocation distribution. A modified version of the Bailey–Orowan equation for simultaneous work-hardening and recovery during constant strain rate deformation which is derived from the model takes the form

$$\theta = H - \eta(t) R/\dot{\varepsilon}$$

where R is the rate of recovery and $\eta(t)$, which is time-dependent during the transient stage of deformation, is determined by such factors as σ, ρ and the details of the dislocation distribution.

1. Introduction

The mechanical properties of crystalline materials are determined largely by the behaviour of dislocations when such materials are subjected to an external stress. The dislocation structure in an annealed crystal typically consists of a three-dimensional array of randomly distributed dislocation segments. Upon the application of stress, the glide motion of dislocations which happen to lie on favourably oriented crystallographic planes results in the production of plastic strain. This is often accompanied by an increase in the density of dislocations and, usually, a perceptible change in the dislocation distribution. Also associated with this process is the phenomenon of work-hardening whereby the applied stress has to be continually increased in order to maintain steady plastic flow. Work-hardening at low temperatures is ordinarily attributed to the increasing interaction between the stress fields of dislocations as their density increases during multiple slip.

The flow stress during classical work-hardening usually varies in direct proportion with the square root of the dislocation density. Several work-hardening theories have been proposed to explain this observation [1, 2]. The correlation between strength and dislocation density, however, usually breaks down in materials deformed at elevated temperatures. During the normal primary stage of recovery creep, the free dislocation density decreases even though the material is becoming stronger, as is manifested by the decreasing creep rate. Such apparent lack of correlation has also been observed in materials deformed under constant strain rate at high temperatures [3, 4]. It is often not possible to correlate high temperature strength with the dislocation structure without invoking subgrain strengthening. This is in spite of several observations of work-softening and creep-weakening which have also been associated with the process of subgrain formation in various materials [5–8].

It is firmly established that, besides work-hardening, recovery also occurs during high temperature deformation, as is evident from such metallographically observable features as the reduction in dislocation density and, sometimes, the formation of a substructure. It is becoming increasingly clear that problems associated with high temperature strength/microstructure correlations will not abate as long as rationalizations of strength are based mainly on the obstacle density, with little consideration for the rate at which such obstacles are overcome. In recovery-controlled deformation, the latter is determined by the rate of recovery, whose effect on the rate of deformation has been so often overlooked apparently because it is not a feature which can be directly observed metallographically.

* On leave from the Department of Physics, Obafemi Awolowo University, Ile-Ife, Nigeria.

0022–2461/91 $03.00 + .12

A recent creep model in which this "dynamic effect" is taken into account establishes a direct correlation between the creep rate and the rate of annihilation of dislocations in a three-dimensional network [9]. In the present paper, the basic ideas of the network recovery model are applied to high temperature constant strain rate deformation in order to place the role of recovery during this deformation mode in proper perspective.

2. Physical background

The so-called "free" dislocations are often arranged in the classical Frank network configuration during high temperature deformation. This consists of randomly-oriented dislocation links of various lengths (λ) which are joined at nodes. Following Lagneborg and co-workers [10–12], the frequency function $\phi(\lambda, t)$ at any instant, t, is defined such that $\phi(\lambda, t)d\lambda$ is the number of links per unit volume having lengths between λ and $\lambda + d\lambda$ (Fig. 1). Under an applied stress, σ, only favourably-oriented links which attain a threshold size λ_a can glide. This threshold size is given by

$$\lambda_a = \alpha_0 Gb/\sigma \tag{1}$$

where G is the shear modulus of the material, b the Burgers vector of the dislocations and α_0 is a constant. The average link length $\langle\lambda\rangle$ is related to the free dislocation density (ρ) according to the equation

$$\langle\lambda\rangle = \rho^{-1/2} \tag{2}$$

A rough cellular structure, consisting mainly of dislocation tangles, rather than a well-defined network, is usually associated with low-temperature deformation. However, within the tangles will be found dislocation segments of various lengths and orientations, and only those with the appropriate threshold length and favourable crystallographic orientation will be able to glide in response to the applied stress. Thus the notion of distribution function as well as the average and threshold link sizes can also be applied to dislocation structures formed during low temperature deformation.

If the stress on a sample deforming at low temperature (i.e. in the absence of recovery) is held constant, deformation stops. This implies that links longer than the threshold size either do not exist, or are otherwise not favourably oriented for glide, in which case they can be considered immobile. Dislocations can be mobilized only by decreasing λ_a (i.e. by increasing σ). This gives rise to the effect known as "work-hardening". Certain past work-hardening models, such as the dislocation meshlength theory, have been formulated along essentially the same conceptual lines [13].

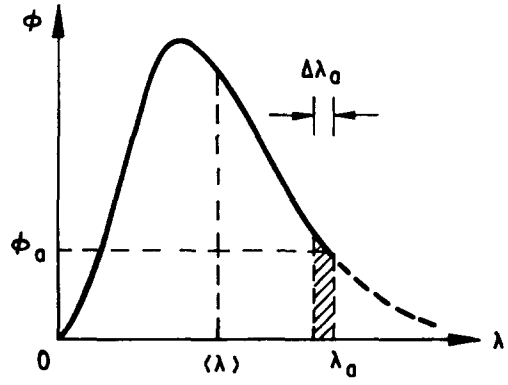

Figure 1 Schematic illustration of the distribution function $\phi(\lambda, t)$ indicating the links which are mobilized upon reducing the threshold size by $\Delta\lambda_a$ (shaded area).

At high temperature the mobilization of dislocations can also be effected through the recovery growth of links to the threshold size. In the creep deformation mode, λ_a is constant due to the constancy of σ while $\langle\lambda\rangle$ increases as the dislocation structure coarsens by recovery. In recovery-controlled (athermal) creep, potentially mobile links which attain the threshold length, λ_a, through recovery are mobilized and the number of such mobilized links per unit time determines the creep rate [9]. It is presumed that dislocations glide "jerkily" which in effect means that they spend a relatively long time waiting to attain the threshold size and, upon attaining it, glide rapidly to the next obstacle. In pure metals and certain solid solutions these obstacles are mainly other network links whose interactions with the gliding links often result in the formation of dislocation nodes. For the kind of (jerky) glide envisaged, most links must, at any instant, be waiting while relatively few are gliding. This means that λ_a must be appreciably larger than $\langle\lambda\rangle$, as shown in Fig. 1 [14]. The thermally activated release of links which could be shorter than λ_a is also possible but is not considered in this model.

3. Low temperature deformation

Upon increasing the applied stress by $\Delta\sigma$, the threshold size decreases by $\Delta\lambda_a$, whereupon $\Delta\rho_m$ dislocations are mobilized (Fig. 1). This is the density of dislocations contained within the shaded region under the distribution curve, and is given by

$$\Delta\rho_m = -f_p\phi_a\lambda_a\Delta\lambda_a \tag{3}$$

where $\phi_a = \phi(\lambda_a, t)$ and the negative sign derives from the fact that a decrease in λ_a is required to mobilize links. Implicit in Equation 3 is the assumption that within any given region in the distribution, a constant fraction f_p of links are favourably oriented for glide. This is the fraction of links which are potentially mobile. The rate of mobilization of links is, from Equation 3

$$\dot{\rho}_m = -f_p\phi_a\lambda_a d\lambda_a/dt \tag{3a}$$

The strain, $\Delta\varepsilon$, generated within a small time interval, Δt, when ΔN_m dislocation links (per unit volume) are mobilized is

$$\Delta\varepsilon = \alpha_1 b\langle A\rangle\Delta N_m \tag{4}$$

where $\langle A\rangle$ is the average area swept by a mobilized link and α_1 is a constant. We can re-write Equation 4 as $\Delta\varepsilon = \alpha_1 bL\lambda_a\Delta N_m = \alpha_1 bL\Delta\rho_m$, where $\Delta\rho_m (= \lambda_a\Delta N_m)$ is the density of links mobilized and $L (= \langle A\rangle/\lambda_a)$ is closely related to the average distance through which a dislocation glides before encountering the next obstacle, or the average obstacle spacing. Thus as

$\Delta t \to 0$, the strain rate becomes

$$\dot{\varepsilon} = \alpha_1 bL\dot{\rho}_m \tag{5}$$

which, combined with Equation 3a gives

$$\dot{\varepsilon} = -\alpha_1 bLf_p\phi_a\lambda_a d\lambda_a/dt \tag{6}$$

Differentiating Equation 1 with respect to t and setting $\alpha_0 Gb = c$ gives

$$\frac{d\lambda_a}{dt} = -\frac{c}{\sigma^2}\frac{d\sigma}{dt} \tag{7}$$

which can be combined with Equations 1 and 6 to yield

$$\dot{\varepsilon} = \frac{\alpha_1 bLf_p\phi_a c^2\dot{\sigma}}{\sigma^3} \tag{8}$$

where $\dot{\sigma} = d\sigma/dt$.

Assuming that dislocation multiplication results mainly from the glide of mobilized links and taking the density of dislocations generated ($\Delta\rho$) within a small time interval (Δt) to vary proportionally with the density mobilized ($\Delta\rho_m$),

$$\Delta\rho = \beta\Delta\rho_m = -\beta f_p\phi_a\lambda_a\Delta\lambda_a \tag{9}$$

where the expression for $\Delta\rho_m$ in Equation 3 has been used and β is a proportionality constant. Noting that $\Delta\lambda_a = -c\Delta\sigma/\sigma^2$ (from Equation 7), Equation 9 becomes, in the limit $\Delta t \to 0$,

$$\frac{d\sigma}{d\rho} = \frac{\sigma^2}{\beta c f_p\phi_a\lambda_a} \tag{10}$$

The relation

$$\sigma = \alpha_2 Gb\rho^{1/2} \tag{11}$$

where α_2 is a constant, is often found to hold during constant strain rate deformation at low temperature. Differentiating Equation 11 gives

$$\frac{d\sigma}{d\rho} = \frac{\alpha_2 Gb}{2\rho^{1/2}} \tag{12}$$

which, when compared with Equation 10 yields, for low temperature deformation,

$$\phi_a = \frac{2\rho^{1/2}\sigma^2}{\beta c\alpha_2 Gbf_p\lambda_a} \tag{13}$$

This expression for ϕ_a appears reasonable as it predicts that the number of threshold-size links should increase with increasing ρ and σ, and decreasing λ_a. By virtue of Equations 1 and 11, Equation 13 gives $\phi_a \propto \rho^2$ during low temperature deformation.

The low temperature work-hardening rate, H, is found by re-arranging Equation 8 to give

$$H = \frac{d\sigma}{d\varepsilon} = \frac{\dot{\sigma}}{\dot{\varepsilon}} = \frac{\sigma^3}{\alpha_1 bLf_p\phi_a c^2} \tag{14}$$

Substituting for ϕ_a (Equation 13) in Equation 14 and taking cognizance of Equation 1, the work-hardening rate can be written as

$$H = (\beta\alpha_2/2\alpha_1)G \tag{15}$$

where L has been assumed to be equal to $\rho^{-1/2}$. Equation 15 predicts linear work-hardening (H = constant), as is observed to be the case during the stage II deformation of single crystals [1, 2]. Since α_1 and α_2 are both of the order of unity, the fact that H is orders of magnitude lower than G simply implies that $\beta \ll 1$. In other words, the fractional increase in length associated with a mobilized link during one glide event must be small.

4. High temperature deformation

Dislocation links are mobilized through the combined action of recovery and stress increase during high temperature deformation. Here we visualize a situation in which the distribution is held stationary for time Δt during which links of threshold size ($\lambda = \lambda_a$) increase their length by $\Delta\lambda|_{\lambda=\lambda_a}$ through recovery. Links lying within the dotted region under the frequency curve (Fig. 2) will be mobilized if glide were now allowed to occur. The density of mobilized dislocations due to recovery alone (i.e. holding σ or λ_a constant) is thus

$$\Delta\rho_{m,r} = f_p\phi_a\lambda_a\Delta\lambda|_{\lambda=\lambda_a} \tag{16}$$

If the applied stress were also to be increased by $\Delta\sigma$ within the time interval Δt during which recovery has occurred, the threshold link size would decrease by $\Delta\lambda_a$, resulting in an additional density of dislocations (the hatched area in Fig. 2) being mobilized. The density, $\Delta\rho_{m,\sigma}$, mobilized through the stress increase is given by Equation 3 or

$$\Delta\rho_{m,\sigma} = -f_p\phi_a\lambda_a\Delta\lambda_a \tag{3a}$$

The total density of dislocations mobilized is (Equations 3a and 16)

$$\Delta\rho_m = \Delta\rho_{m,r} + \Delta\rho_{m,\sigma} = f_p\phi_a\lambda_a(\Delta\lambda|_{\lambda=\lambda_a} - \Delta\lambda_a) \tag{17}$$

In deriving Equation 17 a second order term involving $\Delta\phi_a$ and $\Delta\lambda_a$, which may arise as a result of the

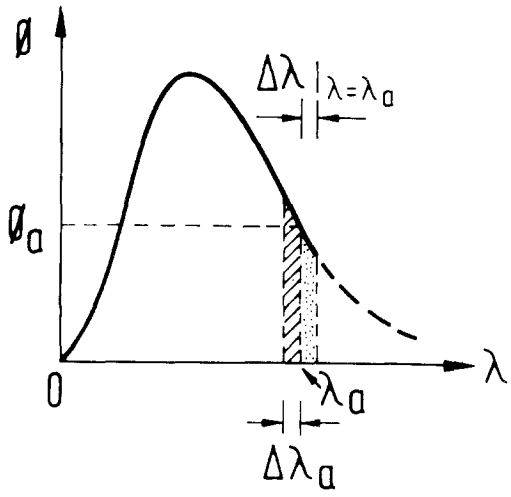

Figure 2 Schematic illustration of the links mobilized due to (a) the recovery–growth of threshold size links by $\Delta\lambda|_{\lambda=\lambda_a}$ (dotted area) and (b) the reduction of the threshold size by $\Delta\lambda_a$ upon stress increase (shaded area).

variability of ϕ with t, has been neglected. The mobilization rate is $\Delta\rho_m/\Delta t$ in the limit $\Delta t \to 0$, or

$$\dot{\rho}_m = f_p \phi_a \lambda_a \left[\left. \frac{d\lambda}{dt} \right|_{\lambda = \lambda_a} - \frac{d\lambda_a}{dt} \right] \quad (18)$$

As the links of threshold size grow by $\Delta\lambda|_{\lambda = \lambda_a}$ during recovery, the whole network coarsens in such a way that the average link size increases by $\Delta\langle\lambda\rangle$. The first term inside the bracket (Equation 18) can be written as

$$\left. \frac{d\lambda}{dt} \right|_{\lambda = \lambda_a} = \psi_o \left. \frac{\partial\langle\lambda\rangle}{\partial t} \right|_\varepsilon \quad (19)$$

where ψ_o is, by definition, the ratio of the growth rate of threshold-size links to the growth rate of the average link size $\langle\lambda\rangle$ [9]. The use of the partial derivative in Equation 19 is to emphasize that the growth of $\langle\lambda\rangle$ referred to here is that which occurs during recovery in the absence of glide (ε is held constant). As demonstrated elsewhere [9], the value of ψ_o depends on certain features of the dislocation distribution, such as the critical link size required for the growth of individual links, as well as the instantaneous values of $\langle\lambda\rangle$ and λ_a. ψ_o is thus expected to be time-dependent as the nature of the distribution changes during deformation.

Differentiating Equation 2 with respect to time gives

$$\left. \frac{\partial\langle\lambda\rangle}{\partial t} \right|_\varepsilon = -\frac{\rho^{-3/2}}{2} \left. \frac{\partial\rho}{\partial t} \right|_\varepsilon$$

whereupon Equation 19 becomes

$$\left. \frac{d\lambda}{dt} \right|_{\lambda = \lambda_a} = \frac{\psi_o \dot{\rho}_a}{2\rho^{3/2}} \quad (20)$$

where $\dot{\rho}_a (= -(\partial\rho/\partial t)_\varepsilon)$ is the annihilation rate of dislocations. Combining Equations 1, 7 and 20 with Equation 18 we have

$$\dot{\rho}_m = \frac{c f_p \phi_a}{\sigma} \left[\frac{\psi_o \dot{\rho}_a}{2\rho^{3/2}} + \frac{c\dot{\sigma}}{\sigma^2} \right] \quad (21)$$

The strain rate is found by substituting this expression for $\dot{\rho}_m$ into Equation 5, giving

$$\dot{\varepsilon} = \frac{\alpha_1 b L c f_p \phi_a}{\sigma} \left[\frac{\psi_o \dot{\rho}_a}{2\rho^{3/2}} + \frac{c\dot{\sigma}}{\sigma^2} \right] \quad (22)$$

Rearranging Equation 22 gives the work-hardening rate, θ, during high temperature deformation, i.e.

$$\theta = \frac{\dot{\sigma}}{\dot{\varepsilon}} = \frac{\sigma^2}{c} \left[\frac{\sigma}{\alpha_1 b L c f_p \phi_a} - \frac{\psi_o \dot{\rho}_a}{2\rho^{3/2}\dot{\varepsilon}} \right] \quad (23)$$

which, in view of Equation 14 can be written as

$$\theta = H - \frac{\psi_o \dot{\rho}_a \sigma^2}{2c\rho^{3/2}\dot{\varepsilon}} \quad (24)$$

Equation 24 gives the relationship between the slope of the high temperature stress–strain curve, θ, and the low temperature work-hardening rate, H. Besides the dependence of θ on the stress, the dislocation density and the strain rate (or cross-head speed), it is also sensitive to $\dot{\rho}_a$ and ψ_o, both of which are influenced by the dislocation distribution [9].

5. The Bailey–Orowan model

In deriving the Bailey–Orowan equation, it is customary to start with the differential equation

$$d\sigma = H d\varepsilon - R dt \quad (25)$$

where $H (= (\partial\sigma/\partial\varepsilon)_t)$ is the work-hardening rate and $R (= -(\partial\sigma/\partial t)_\varepsilon)$ is the rate of recovery. It follows from Equation 25 that

$$\theta = H - R/\dot{\varepsilon} \quad (26)$$

The exact differential (Equation 25) could only come from a mechanical equation of state such as $\sigma = \sigma(\varepsilon, t)$, the validity of which has been called into question [15]. Attempts by past workers to fit constant strain-rate deformation data on various materials into Equation 26 have also proved futile [16, 17]. Based on the present model, an equation is derived below for θ which, though similar in form to Equation 26, bears a significant difference.

If a pre-deformed sample is recovered at high temperature and subsequently re-tested at low temperature, the flow stress is expected to decrease as a result of the reduction in the dislocation density, in conformity with Equation 11. Suppose the low temperature flow stress, σ, changes by $-\Delta\sigma$ upon recovering for time Δt at high temperature.

From Equation 11

$$-\left[\frac{\Delta\sigma}{\Delta t} \right]_\varepsilon = -\frac{\alpha_2 G b}{2\sqrt{\rho}} \left[\frac{\Delta\rho}{\Delta t} \right]_\varepsilon \quad (27)$$

where $\Delta\rho$ is the change in the dislocation density due to recovery and the subscript ε indicates that recovery is carried out in the absence of glide. In the limit $\Delta t \to 0$, the left hand side of Equation 27 is the rate of recovery, or

$$R = -\left[\frac{\partial\sigma}{\partial t} \right]_\varepsilon = \frac{\alpha_2 G b \dot{\rho}_a}{2\rho^{1/2}} \quad (28)$$

Combining Equation 28 with 24 yields

$$\theta = H - \frac{\alpha_o \psi_o \sigma^2 R}{\alpha_2 c^2 \rho \dot{\varepsilon}} \quad (29)$$

or

$$\theta = H - \eta(t) R/\dot{\varepsilon} \quad (30)$$

where

$$\eta(t) = \alpha_o \psi_o \sigma^2/(\alpha_2 c^2 \rho) \quad (31)$$

Equation 30 is similar in form to Equation 26 with the important difference that the former contains a function $\eta(t)$ which depends on the applied stress, the dislocation density and the dislocation distribution (through ψ_o).

The implications of the network model for the Bailey–Orowan equation as applicable to creep deformation have been discussed elsewhere [18]. It is demonstrated therein that the equation $\dot{\varepsilon} = R/H$ is valid for steady-state but not for transient creep. This implies naturally that it is also valid for the steady-state stage of constant strain rate deformation, in which case $\eta(t)$ must be equal to 1, i.e. from Equation 31

$$\sigma = \alpha_3 G b \rho^{1/2} \quad (32)$$

where $\alpha_3 = (\alpha_0\alpha_2/\psi_0)^{1/2}$. The direct proportionality between σ and $\rho^{1/2}$ (Equation 32) during steady-state deformation is well established, be it under the creep or the constant strain rate mode.

6. Comparison with experimental data

Figs 3 and 4 show the σ vs ε and ρ vs ε data obtained by Przystupa *et al.* [4] for NaCl monocrystals deformed under compression at 873 K and 973 K. The flow stress, σ, increases monotonically with strain even though the free dislocation density, ρ, goes through a maximum at an early stage of deformation (about 2% strain). These data have been fitted into Equation 29 re-written in the form

$$\psi_0 R = \frac{(H - \theta)\dot{\varepsilon}c^2\alpha_2\rho}{\alpha_0\sigma^2} \qquad (29a)$$

The values of σ and θ (the slope) are taken from the longest curves in Fig. 3, which are also fairly representative of the stress–strain behaviour at each of the two test temperatures; ρ is taken from the data of Fig. 4.

Since the cross-head velocity was held constant, the true strain rate, $\dot{\varepsilon}$, during the compression tests varied according to the expression

$$\dot{\varepsilon} = 6.94 \times 10^{-5}\exp|\varepsilon|\ s^{-1} \qquad (33)$$

which means that $\dot{\varepsilon}$ increased from $7.01 \times 10^{-5}\ s^{-1}$ to $8.48 \times 10^{-5}\ s^{-1}$ as ε increased from 0.01 to 0.20 [4]. The value of $\dot{\varepsilon}$ evaluated at each strain level is used in Equation 29a. The following values of the other parameters appearing in the equation are also used

$\alpha_0 \simeq \alpha_2 = 0.5$

$b = 3.97 \times 10^{-10}$ m for NaCl

$G = 9.5 \times 10^9\ Nm^{-2}$ at 873 K and $8.4 \times 10^9\ Nm^{-2}$ at 973 K [4]

$c = \alpha_0 Gb = 1.89\ Nm^{-1}$ at 873 K and $1.67\ Nm^{-1}$ at 973 K.

The value of the work-hardening rate H used to fit the data is $1.5 \times 10^7\ Nm^{-2}$, or $H/G \simeq 1/600$, which falls within the range of commonly observed H/G values [2] and is also close to the value ($\sim 10^7\ Nm^{-2}$) reported by Schmitten and Haasen for NaCl monocrystals deformed at room temperature [19].

The values of the quantity $(\psi_0 R)$ obtained from Equation 29a are plotted as a function of strain in Fig. 5 for each of the two test temperatures. If the time (and hence strain) dependence of ψ_0 is assumed to be relatively mild, the curves in Fig. 5 can be interpreted as the mode of variation of the rate of recovery during deformation. These curves bear striking similarity to the ρ vs ε curves (Fig. 4), suggesting a direct correlation between the recovery rate and the dislocation density.

The stress–strain curves can be rationalized as follows. The slope, θ, of each curve decreases as the quantity $(\sigma^2/\rho)(\psi_0 R)$ increases (Equation 29). In the early stage of deformation ($\varepsilon < 2\%$), the dislocation

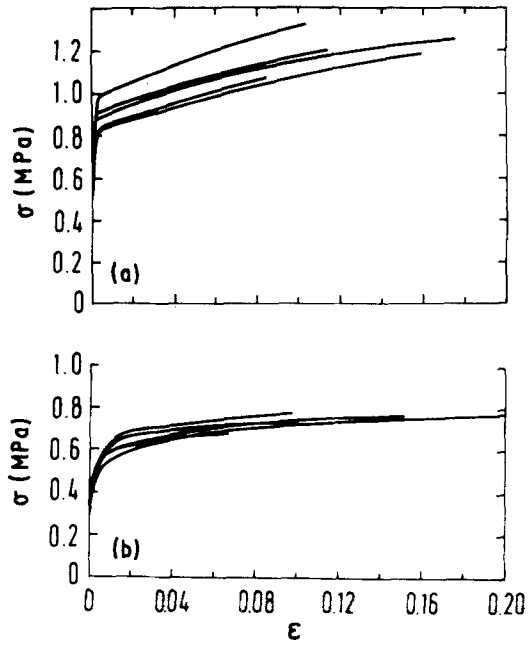

Figure 3 Stress–strain curves for NaCl single crystals deformed under constant crosshead speed at 873 K (a) and 973 K (b) [4].

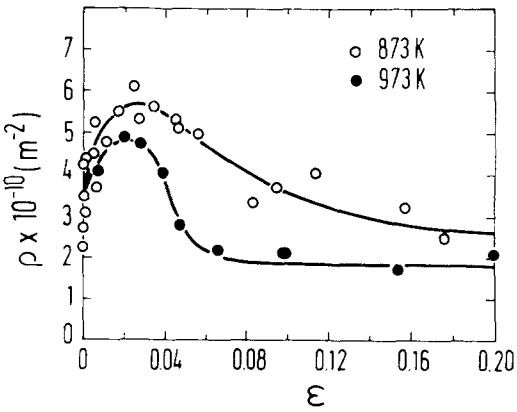

Figure 4 Variation of free dislocation density, ρ, with strain, ε, for NaCl single crystals deformed at 873 K (○) and 973 K (●) [4].

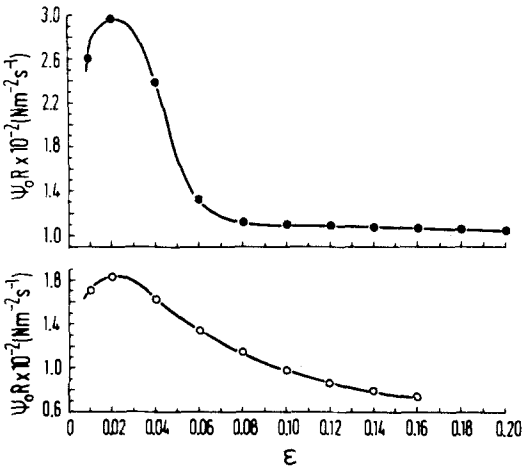

Figure 5 Plots of $(\psi_0 R)$ against ε at 873 K (○) and 973 K (●).

density increases following yield and the rate of recovery increases correspondingly. The decrease in slope of the stress–strain curve results largely from the increasing contribution of recovery to the mobilization of dislocation links of threshold size. With the

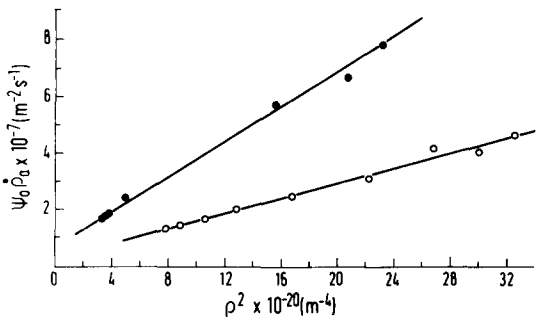

Figure 6 Plots of $(\psi_0\dot{\rho}_a)$ against ρ^2 at 873 K (○) and 973 K (●).

annihilation of some of the dislocations and the rearrangement of others into low angle boundaries ($\varepsilon > 2\%$), the free dislocation density starts decreasing and is accompanied by a reduction in the rate of recovery. The fact that the slope, θ, keeps decreasing beyond the peak dislocation density implies that the ratio σ^2/ρ increases faster than $\psi_0 R$ decreases, which is not surprising since σ increases while ρ decreases.

From Equation 28, we can write

$$\psi_0\dot{\rho}_a = \frac{2(\psi_0 R)\rho^{1/2}}{\alpha_2 Gb} \tag{34}$$

Values of $\psi_0\dot{\rho}_a$ obtained from Equation 34 using the $\psi_0 R$ values from Equation 29a are shown plotted against ρ^2 in Fig. 6 for $T = 873$ K and 973 K. The plot is linear, i.e.

$$\psi_0\dot{\rho}_a = k\rho^2 \tag{35}$$

where the slope, k, which is related to the mobility and line tension of dislocations [20], is equal to $1.32 \times 10^{-14}\,m^2\,s^{-1}$ at 873 K and $3.08 \times 10^{-14}\,m^2\,s^{-1}$ at 973 K. The annihilation rate can thus be written as

$$\dot{\rho}_a = kf(t)\rho^2 \tag{36}$$

where $f(t) = 1/\psi_0$. This function can be attributed to the time dependence of the distribution function [9] and the flow stress in the experiments under consideration. Recovery experiments are in progress to confirm these observations.

7. Discussion and conclusions

From Equation 30 it is seen that a material subjected to constant strain rate deformation could display positive work-hardening, zero work-hardening or negative work-hardening (work-softening) depending on the relative values of the parameters appearing in the equation. Thus work-hardening ($\theta > 0$) is expected at high strain rates or when recovery is slow, and work-softening ($\theta < 0$) at low strain rates or when recovery is rapid. Zero work-hardening ($\theta = 0$) occurs when a balance is struck between the "recovery parameters" on the one hand and the work-hardening rate on the other, i.e. when $H = \eta(t)R/\dot{\varepsilon}$. This corresponds to either a peak in the stress–strain curve or the steady-state configuration. At steady-state, Equation 23, when rearranged to make $\dot{\varepsilon}$ the subject, becomes identical to the expression for the creep rate for a material tested in the creep mode [9].

The fact that H is always positive during low temperature deformation is a natural consequence of the constraint of an imposed (constant) strain rate. If the stress on a sample deforming at low temperature is held constant, generation of plastic strain will stop as soon as all links of threshold size have moved and got re-arrested at the nearest obstacles. Following the exhaustion of the threshold-size links, further mobilization of links is possible only if a new (shorter) threshold size is established, which in effect means that the stress must be increased (work-hardening).

At high temperature, the generation of plastic strain continues even when the stress is constant. This *creep* deformation occurs because the continuous supply of new sources of slip (i.e. links of threshold size) is assured by the recovery growth of the network links. The rate of supply of such links, and thus the creep rate, depend on the rate of recovery. During constant strain rate deformation, the rate of supply of threshold-size links cannot cope with the imposed strain rate if the stress is held constant and recovery is too slow. The stress must therefore be increased ($\theta > 0$) so as to reduce the threshold size and mobilize more links. As recovery speeds up, the rate of annihilation may reach the critical value where the supply of threshold-size links through recovery becomes just sufficient to conform with the imposed strain rate. Under this condition deformation continues without an increase in stress ($\theta = 0$).

Under very high rates of recovery, the rate of mobilization of links by recovery may become higher than can be accommodated by the imposed strain rate, whereby the stress drops ($\theta < 0$). This, in effect, increases the threshold size and reduces the number of movable links. This explains the work-softening commonly observed in materials which are deformed under constant strain rate at high temperature following prestraining at low temperature [6–8]. Cold worked structures are known to be more susceptible to recovery than structures obtained by deformation at high temperatures [8].

The scenario presented in this model shows that recovery influences high temperature deformation in two important ways, of which the reduction in obstacle (i.e. dislocation) density is the more apparent and the widely recognized. The other effect, which is subtle yet profound, is a "dynamic" one in the sense that it is not readily discernible from a visual examination of the instantaneous or "static" dislocation structure. This is the influence of recovery on the rate of production of threshold-size links, which act as new slip sources. The importance of the latter factor stems largely from the nature of dislocation glide in pure metals and some solid solution alloys: in a situation where most of the links are held up in the network at any given instant, it is to be expected that the rate of deformation may be determined more by the rate of mobilization of links than by the details of the glide process itself.

This model and its creep counterpart developed earlier [9] have shown clearly that the mechanism of high temperature deformation is fundamentally the same, be it under the condition of constant strain rate

or constant stress (creep). The main difference lies in the externally imposed constraints. In the former, the sample complies with an imposed strain rate as new slip sources are activated through recovery, and, if necessary, through stress adjustments, while in the latter, an imposed stress constrains the sample to deform at a rate which is dictated largely by the speed of recovery. Whereas work-hardening denotes the inability of recovery to cope with the imposed strain rate in the one case; in the other, the declining strain rate (during normal transient creep) is a manifestation of the decreasing rate of mobilization of links due to the decreasing rate of recovery.

References

1. F. R. N. NABARRO, Z. S. BASINSKI and D. B. HOLT, Advances in Phys. **13** (1964) 193.
2. H. M. OTTE and J. J. HREN, *Experimental Mech.* **6** (1966) 177.
3. J. N. McCORMICK, Ph.D. thesis, University of California, Los Angeles (1977).
4. M. A. PRZYSTUPA, P. LIN, A. J. ARDELL and O. AJAJA, *Mater. Sci. Engr.* **92** (1987) 63.
5. O. AJAJA and A. J. ARDELL, *Phil. Mag.* **A39** (1979) 65.
6. W. P. LONGO and R. E. REED-HILL, *Scripta Metall.* **4** (1970) 765.
7. B. BRENNER and A. LUFT, *Mater. Sci. Engr.* **52** (1982) 229.
8. T. H. ALDEN, *Metall. Trans.* **7A** (1976) 1057.
9. O. AJAJA, *J. Mater. Sci.* **21** (1986) 3351.
10. R. LAGNEBORG and B. H. FORSEN, *Acta Metall.* **21** (1973) 781.
11. P. OSTROM and R. LAGNEBORG, *J. Eng. Mater. Tech.* **98** (1976) 114.
12. P. OSTROM and R. LAGNEBORG, *Res. Mechanica* **1** (1980) 59.
13. D. KUHLMANN-WILSDORF, Trans. TMS-AIME **224** (1962) 1047.
14. J. B. FAGBULU and O. AJAJA, *J. Mater. Sci. Lett.* **6** (1987) 894.
15. O. AJAJA, *Res. Mechanica* **10** (1984) 79.
16. H. MECKING, U. F. KOCKS and H. FISCHER, in Proceedings of the Fourth International Conference on the Strength of Metals and Alloys (France, 1976) p. 334.
17. J. L. ROUTBORT, *Acta Metall.* **27** (1979) 649.
18. S. O. OJEDIRAN and O. AJAJA, *J. Mater. Sci.* **23** (1988) 4037.
19. W. in der SCHMITTEN and P. HAASEN, *J. Appl. Phys.* **32** (1961) 1790.
20. R. LAGNEBORG, B. H. FORSEN and J. WIBERG, Proceedings of the Meeting on Creep Strength in Steel and High-Temperature Alloys, Sheffield (Sheffield, Iron and Steel Inst., 1972) p. 1.

Received 4 December 1989
and accepted 6 November 1990